



Science Arts & Métiers (SAM)

is an open access repository that collects the work of Arts et Métiers Institute of Technology researchers and makes it freely available over the web where possible.

This is an author-deposited version published in: <https://sam.ensam.eu>
Handle ID: <http://hdl.handle.net/10985/12895>

To cite this version :

Shabab SAMIMI, Philippe DELARUE, Frédéric COLAS, Mohamed Moez BELHAOUANE, Xavier GUILLAUD, Francois GRUSON - MMC Stored Energy Participation to the DC Bus Voltage Control in an HVDC Link - IEEE Transactions on Power Delivery - Vol. 31, n°4, p.1710-1718 - 2016

Any correspondence concerning this service should be sent to the repository

Administrator : scienceouverte@ensam.eu



MMC Stored Energy Participation to the DC Bus Voltage Control in an HVDC Link

Shabab Samimi, Francois Gruson, Philippe Delarue, Frederic Colas, Mohamed Moez Belhaouane,
Member, IEEE, Xavier Guillaud, Member, IEEE

Abstract—The Modular multilevel converter (MMC) is becoming a promising converter technology for HVDC transmission systems. Contrary to the conventional two or three level VSC-HVDC links, no capacitors are connected directly on the DC bus in an MMC-HVDC link. Therefore, in such an HVDC link the DC bus voltage may be much more volatile than in a conventional VSC-HVDC link. The intention of this paper is to propose a connection between the DC bus voltage level and the stored energy inside the MMC in order to greatly improve the dynamic behavior in case of transient. EMT simulation results illustrate this interesting property on an HVDC link study case.

Index Terms— Electromagnetic Transients program (EMTP), HVDC, Modular Multilevel Converter, MMC, Energy and power control.

I. NOMENCLATURE

As shown in Fig 1, the upper and lower arm components are denoted with the subscripts “u” and “l” respectively. In the expressions, “i” is the phase index: phase a, phase b and phase c. The index “ref” denotes the references. The main MMC parameters and variables are listed as follows:

SM	Sub Module.
C	SM capacitance.
$C_{tot i}$	Equivalent Arm capacitance.
C_{dc}	Cable capacitance.
m_{uli}	Arm duty cycle
$v_{mul i}$	Arm modulated voltage
$i_{mul i}$	Equivalent arm capacitor current
$i_{ul i}$	Per-arm current
$v_{cul i_tot}$	Equivalent arm capacitor voltage.
i_{gi}	ac grid current.
v_{gi}	ac grid voltage.

$i_{diff i}$	Circulating current.
v_{vi}	Internal voltage (driving i_{gi}).
$v_{diff i}$	Internal voltage (driving $i_{diff i}$).
W_i^Σ	Per-phase stored energy
W_i^Δ	Difference stored energy between phase-arms.
W_{tot}	Total 3-phases stored energy
$p_{ac i}$	Average per-phase active power.
p_{ac}	Total 3-phases active power.
$p_{dc i}$	Per-phase dc power.
R_{arm}, L_{arm}	Arm resistance and inductance.

II. INTRODUCTION

HVDC power transmission systems can expect large development due to the increasing need to transmit electrical power. Until now, most of the projects have been developed with the classical thyristor technology. Other projects are now under development with the transistor technology, thanks to the use of multilevel voltage source converters (VSCs). Among various multilevel topologies, the fairly recently proposed modular multilevel converter (MMC) is the most promising for high power and high voltage applications, particularly for HVDC links [1, 2]. Fig. 1 recalls a schematic representation of a three phase MMC.

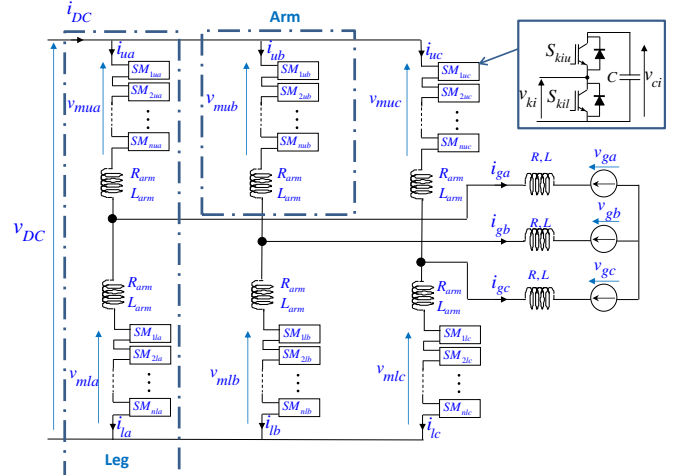


Figure 1: Schematic representation of MMC

Manuscript submitted July 23, 2015;

Shabab Samimi, Prof. Xavier Guillaud Moez Belhaouane are with the L2EP-Ecole Centrale de Lille (email: shabab.khorgami@ec-lille.fr, xavier.guillaud@ec-lille.fr, mohamed-moez.belhaouane@ec-lille.fr), Francois Gruson and Frederic Colas are with L2EP-Arts et Metier Paris Tech (emails: francois.gruson@ensam.eu, frederic.colas@lille.ensam.fr), Philippe Delarue is with L2EP - Polytech, University of Lille (email: philippe.delarue@univ-lille.fr) www. http://l2ep.univ-lille1.fr/

The MMC studied offers some specific advantages over conventional two-level and three-level VSC- HVDC: lower switching losses, higher output voltage level, smaller harmonic component [1-3] and no simultaneous switching between several transistors. This topology is modular and is easily scalable. As illustrated in Fig.1, it consists in N identical series-connected submodules (SMs) based on IGBT.

For HVDC systems, it may include thousands of power switches for the whole converter. In the past few years, significant effort has been made to overcome the technical challenges associated with the modeling and the control of an MMC; a review is provided in [4].

Focusing on the high-level control, current, voltage and energy control, two main solutions are proposed: non-energy based control strategies [5-7], and energy-based control strategies [8-11]. In some publications, the proposed control is applied in an HVDC link [12, 13] but they do not explicitly address the two different roles that are held by this converter in an HVDC link: controlling the power or controlling the DC voltage level as discussed in [12-14].

Looking at both systems in Fig. 2 reveals a fundamental difference in terms of energy localization. In case of a classical VSC, (see Fig. 2a) the capacitor is placed on the DC bus, which means that the storage level depends on the DC voltage. In other words, these storage elements naturally participate in the dc bus voltage stability. In case of an MMC, (see Fig. 2b) the storage elements are inside the converter [1], and no direct link exists with the dc bus. The only storage element on the dc-bus is the dc cable capacitor. In case of a large variation of power on the d bus, this could lead to a very volatile dc voltage.

This paper aims to establish a link between the energy stored in the MMC and the dc bus voltage. The equivalent capacitor seen on the dc bus is greatly increased, which significantly decreases the dc bus variation in case of transient on the power that flows through the MMC substations. A simple solution, called CCSC, already exists but it leads to unwanted oscillations during the transient.

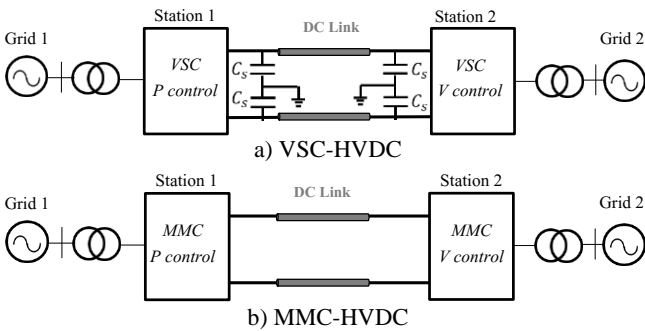


Figure 2: Schematic representation of an HVDC link: a) VSC-HVDC link and b) MMC-HVDC link

This paper is organized as follows: Section III introduces the now classical average arm model [15]. Adding the grid and differential loops gives another level of representation for the MMC, called equivalent energy-based model. From this model, the MMC-power substation control is designed in section IV. In section V, the variable dc bus voltage is

considered, and a link is created between the energy level and the dc bus voltage to allow a contribution of the MMC stored energy to the dc bus voltage regulation. In section VI a comparison between different control schemes and their effects on the dynamic behavior of an MMC HVDC link is presented.

III. MMC MODELLING AND CURRENT CONTROL

A. Average Arm Model

Since only the current and energy control is addressed in this paper, the average arm model is applied in the following sections.

Fig. 3 shows an MMC equivalent model based on the average arm model [16, 17], where it is considered that the balancing of the SM voltage works properly ($v_{c1}=v_{c2}=\dots=v_{cN}$) and the arm's SMs have been replaced by an equivalent model composed of a chopper and an equivalent capacitor. This equivalent capacitor is equal to the sum of all the SM capacitors. If there is N SMs in each arm then this equivalent capacitor (C_{tot}) is equal to C/N capacitance. The voltage applied to this equivalent capacitor is the sum of all the voltages of each SM $v_{cul_i_tot}=v_{c1}+v_{c2}+\dots+v_{cN}$. It is important to notice that in HVDC applications N is several hundred. A duty cycle is defined for the 6 arms ($m_{ua}, m_{ub}, m_{uc}, m_{la}, m_{lb}, m_{lc}$). Each chopper may be modelled as:

$$v_{mul\ i} = m_{ui} v_{cul\ tot\ i}, \quad i_{mul\ i} = m_{ui} i_{ui} \quad (1)$$

$$i_{mul\ i} = C_{tot} \frac{dv_{cul\ i_tot}}{dt} \quad (2)$$

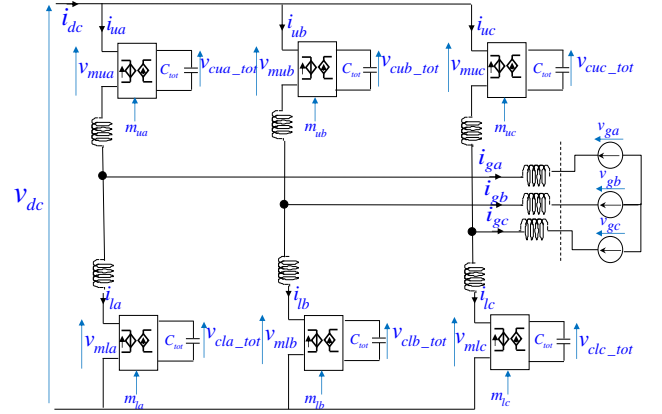


Figure 3: MMC equivalent model

In this model, MMC is characterized by 11 independent state variables: the six equivalent capacitor voltages and 5 currents (three arm currents and two phase currents). The modelling is oriented by performing the classical change of variables:

$$i_{diff\ i} = \frac{i_{ui} + i_{li}}{2}, \quad v_{diff\ i} = \frac{v_{mui} + v_{mli}}{2}, \quad v_{vi} = \frac{v_{mli} - v_{mui}}{2} \quad (3)$$

$$i \in (a, b, c)$$

By these circuit definitions, the description of the system can be split into two sets of decoupled equations:

$$v_{vi} - v_{gi} = (L + \frac{L_{arm}}{2}) \frac{di_{gi}}{dt} + (R + \frac{R_{arm}}{2}) i_{gi} \quad (4)$$

$$\text{With } i_{ga} + i_{gb} + i_{gc} = 0.$$

$$\frac{v_{dc}}{2} - v_{diff i} = L_{arm} \frac{di_{diff i}}{dt} + R_{arm} i_{diff i} \quad (5)$$

The differential currents ($i_{diff a}$, $i_{diff b}$, $i_{diff c}$) are composed of a dc component ($i_{diff i_dc}$) and harmonic components. In normal operations, the sum of the dc components is the dc current delivered to the dc bus. The harmonic currents, which are exchanged between the different legs, can be classified as follows:

- The fundamental component ($i_{diff i_AC}$) which allows balancing between the upper and lower arm voltage [9, 11],
- The circulation currents exchanged between the different legs, which is related to the voltage capacitor fluctuations.

B. MMC current control loops

From (4) and (5), it is possible to design the grid and differential current controls independently.

For the grid current, a classical d,q control may be implemented. In case of an energy-based control, dc and fundamental ac components of the differential current are controlled per phase. More details for current loops can be found in [18] Fig.4 presents a simulation model of the MMC with its current control. The inputs are: the references of the grid currents ($i_{gd\ ref}$, $i_{gq\ ref}$) and the reference of DC and ac component of the differential currents ($i_{diff i_DC\ ref}$, $i_{diff i_AC\ ref}$). The outputs are the arm capacitor voltages (v_{culi_tot}), the grid currents (i_{gi}) and differential currents (i_{diff}).

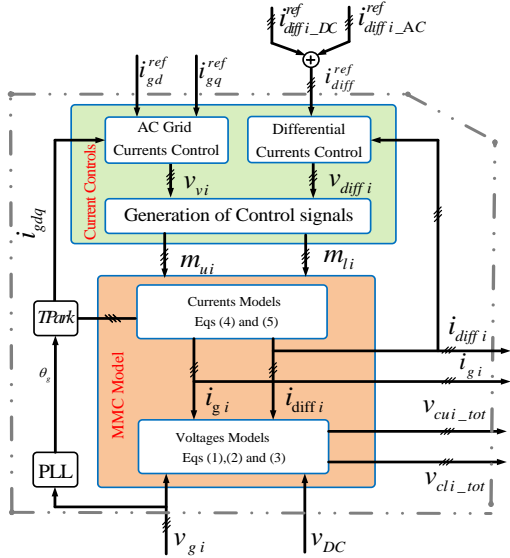


Figure 4: MMC simulation model with the current loops

C. Energy-based model of the MMC

The grid current references are derived from active and reactive power control. In energy-based control, the differential current references are derived from the energy controllers. Two types of energy variables are to be managed: W_i^Σ and W_i^Δ . Both energetic variables depend on v_{cui_tot} and v_{cli_tot} as :

$$W_i^\Sigma = \frac{1}{2} C_{tot} (v_{cui_tot}^2 + v_{cli_tot}^2) \quad (6)$$

$$W_i^\Delta = \frac{1}{2} C_{tot} (v_{cui_tot}^2 - v_{cli_tot}^2) \quad (7)$$

In [19], it has been demonstrated that W_i^Σ can be controlled by the dc component of the differential current and W_i^Δ by the ac component of the differential current. All the different loops are represented in Fig. 5a.

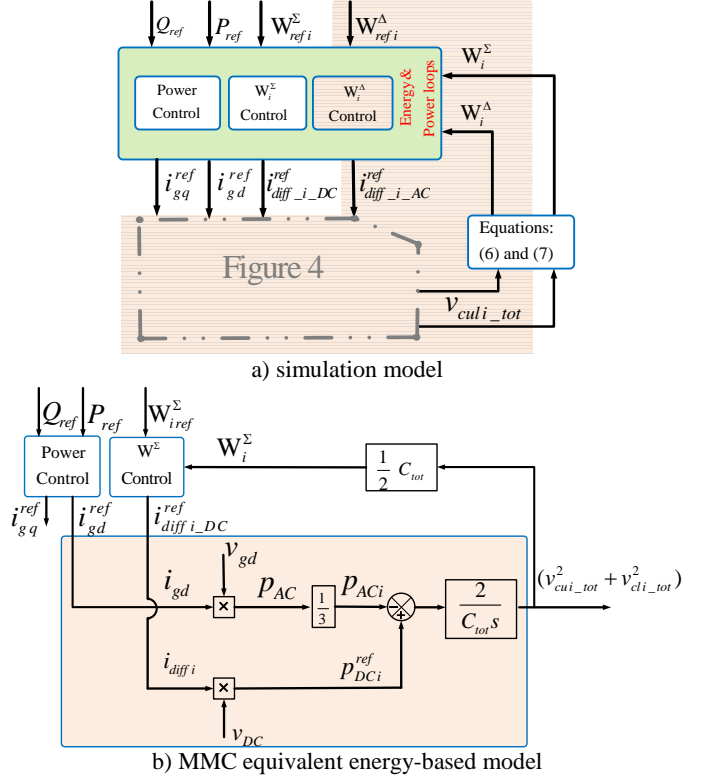


Figure 5: MMC with power and energy loops: a) MMC simulation model, b) MMC equivalent energy-based model

Since only the management of W_i^Σ is addressed, a simplified model is proposed to design the control. The current control loop dynamics are supposed to be infinite which means that: $i_{diff i_DC\ ref} \cong i_{diff i}$ and $i_{gd\ ref} \cong i_{gd}$.

The control of the W_i^Δ is assumed to be independent from the control of W_i^Σ . It will not be taken into consideration in the simplified model.

As shown in [9] W_i^Σ depends on $p_{ac i}$ and $p_{dc i}$:

$$\frac{dW_i^\Sigma}{dt} = \frac{1}{2} C_{tot} \left(\frac{dv_{cui_tot}^2}{dt} + \frac{dv_{cli_tot}^2}{dt} \right) = p_{dc i} - p_{ac i} \quad (8)$$

With:

$$p_{AC i} = \frac{p_{ac}}{3} \quad (9)$$

$$p_{DC i} = v_{DC} i_{diff i} \quad (10)$$

The expression of the whole ac power is given by:

Then the block diagram of the MMC can be modified as shown in Figure 8.

2) Two different ways for the DC Voltage Control

Since the energy is controlled thanks to the DC power, the DC-bus voltage is controlled by the active power reference $P_{AC\ ref}$. To design the DC voltage controller, a link between $P_{AC\ ref}$ and v_{DC}^2 is needed. Adding the set of three equations of (8) leads to the following equation:

$$\frac{dW_{tot}}{dt} = \frac{1}{2} C_{tot} \left(6 \frac{dv_{c\ tot}^2}{dt} \right) = p_{DC} - p_{AC} \quad (14)$$

$$\text{With: } v_{c_tot}^2 = \left(\sum_{i=1}^3 v_{cui_tot}^2 + \sum_{i=1}^3 v_{cli_tot}^2 \right) \quad (15)$$

This equation may be modified by replacing p_{AC} by $P_{AC\ ref}$ and v_{ctot}^2 by $v_{ctot\ ref}^2$

$$\frac{dW_{tot}}{dt} = \frac{1}{2} C_{tot} \left(6 \frac{dv_{c\ tot\ ref}^2}{dt} \right) = p_{DC} - P_{ACref} \quad (16)$$

Merging (18) and (13) results in:

$$\frac{1}{2}C_{DC}\frac{dv_{DC}^2}{dt} = -\frac{1}{2}C_{tot}\left(6\frac{dv_{c\ tot\ ref}^2}{dt}\right) - P_{ACref} + p_l \quad (17)$$

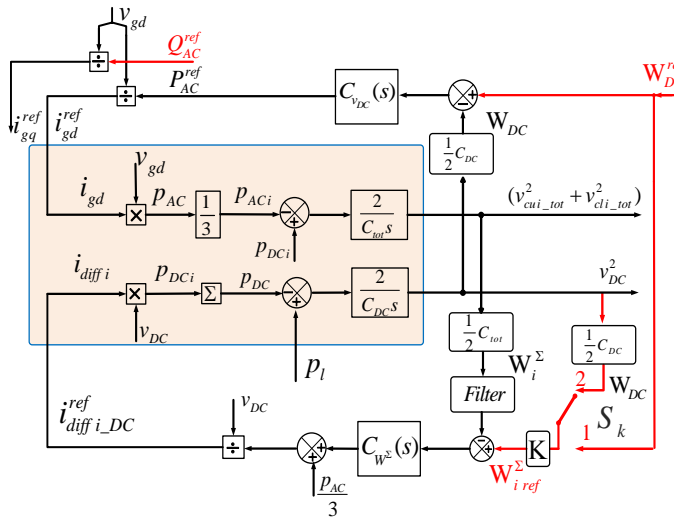


Figure 8: Block diagram of an MMC with DC voltage control

When the switch S_k (see Fig. 8), is in position 1 $W_{iref}^\Sigma = W_{DCref}$, the level of MMC stored energy is constant in a steady state. That is the case usually used in literature. In this case (17) can be written as:

$$\frac{1}{2}C_{DC}\frac{dv_{dc}^2}{dt} = -P_{AC\ ref} + p_l \quad (18)$$

When S_k is in position 2, ($W_{iref}^\Sigma = KW_{DC}$), the level of stored energy in the MMC is related to the level of the DC voltage. In this case (17) may be written as:

$$\frac{1}{2}(6KC_{tot} + C_{DC})\frac{dv_{DC}^2}{dt} = -P_{AC\ ref} + p_l \quad (19)$$

For the CCSC control, v_{ctot} is equal to v_{DC} , (19) is also valid with $K=1$ as shown in [22].

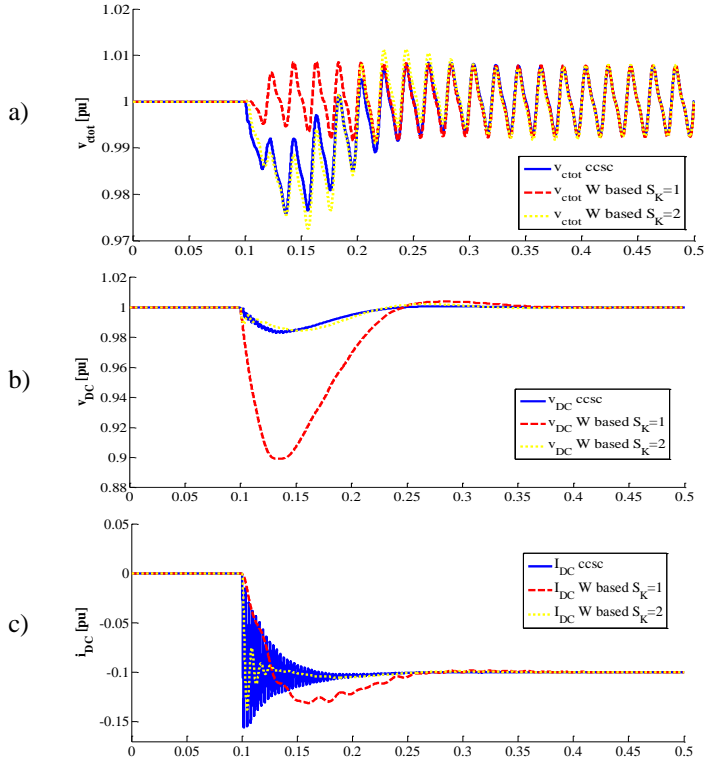
Equation (19) shows that the equivalent capacitor for the regulation of the DC bus now integrates the capacitors of MMC, which induces a high increase for the capacitor value. For example, in this case study the value of the MMC capacitors ($6C_{\text{tot}}$) is 24 times the value of a 70-km DC cable capacitor.

3) Simulation results

In this part, three control solutions are simulated (cf. Fig. 9).

- Non Energy based control, mentioned in section IV,
- Energy based control with a constant energy reference $S_k=1$,
- Energy based control with a variable energy reference $S_k=2$, $K=1$.

The control of the DC-bus voltage is added to each control scenario mentioned in section IV. The simulation results are observed after the following event: Step of -0.1 pu at $t = 0.1$ s a on p_i . The response time of the current and energy loops is the same as in section IV. The DC voltage response time is set at 100 ms.



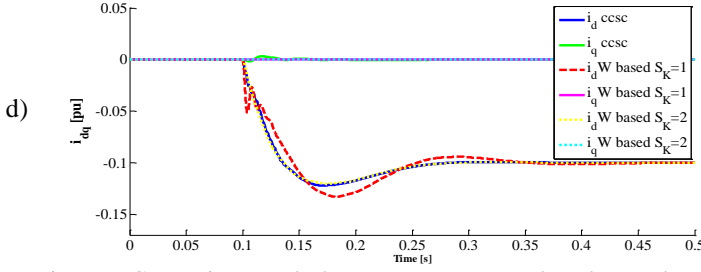


Figure 9: Comparison results between a non-energy based control and energy-based control with variable DC-bus voltage in two cases $S_k = 1$ and $S_k = 2$: a) Total capacitor voltage of the upper arm of phase -a b) DC-bus voltage . c) DC side current, d) dq components of the AC side currents.

Fig. 9a shows that the average value of v_{cutot} follows the DC-bus voltage variation in the non-energy based control scheme, whereas it depends on S_k in the energy-based control scheme.

- $S_k = 1$: v_{cutot} is independent of the DC-bus voltage variation.
- $S_k = 2$: v_{cutot} follows the DC-bus voltage variation

Fig. 9b verified that in the energy-based control scenario, the v_{DC} variation was more significant when $S_k = 1$ than when $S_k = 2$. Indeed, when $S_k = 1$, this variation depends only on the capacitor of the DC cable, as presented in (20).

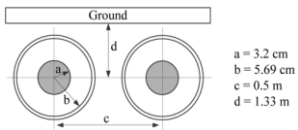
When $S_k = 2$, the equivalent capacitor is equal to $6C_{tot} + C_{DC}$ as presented in (21), the voltage variation is largely decreased. In CCSC, the DC voltage behavior is nearly the same as in the energy-based control with $S_k = 2$. However, the energy is not controlled, and many oscillations are observed on the DC current. On the contrary, the DC current is well damped in the energy-based control (Fig. 9c).

These simulation results clearly show that the proposed control merges two main properties: increased equivalent DC bus capacitor and full control of the DC current.

VI. APPLICATION OF THE PROPOSED CONTROL SYSTEM IN AN HVDC LINK

The proposed control is now applied in a two-terminal HVDC system. The studied HVDC link is shown in Fig.11. The electrical circuit parameters considered for the DC cable are given in Table 2[23].

Table 2: DC cable parameters



Cable length	70 km
Outer radius of sheath	5.82 cm
Outer radius of insulation	6.39 cm
Resistivity of core	$1.72e - 8 \Omega m$
Resistivity of sheath	$2.83e - 8 \Omega mm$
Insulator relative permittivity	2.5
Insulator loss factor	0,0004

As shown in Fig. 12, the MMC stations have two explicitly different roles: Substation 1 controls the power flowing into

this link thanks to the reference signal: P_{AC1ref} . Substation 2 controls the DC voltage level. The design of the voltage controller depends on the equivalent capacitor on the DC bus, which depends on the control applied on both substations.

In order to validate the findings, three simulated case studies evaluate the dynamic performance of the DC bus voltage under the following simulation event: at $t = 0.1s$ a step of 0.1 pu is applied on P_{AC1ref} .

A. Case A: One station with $W_{iref}^\Sigma = KW_{DC}(S_{K1} = 2)$ the other one with $W_{iref}^\Sigma = W_{DCref}(S_{K1} = 1)$

In this case, the W_{iref}^Σ of the MMC station controlling the DC bus voltage is connected to the W_{DC} measurement.

Hence, only the SM capacitors of station 2 participate in the DC voltage control. Equation (19) is adapted to a new configuration: the DC power of substation 1 is substituted by p_l as written in:

$$\frac{1}{2}(6C_{totMMC2} + C_{DC}) \frac{dv_{DC}^2}{dt} = -P_{AC2ref} - p_{DC1} \quad (20).$$

Since W_{tot1}^Σ is constant $P_{AC1ref} \approx p_{DC1}$.

The variation of the DC voltage is considered following a step of 0.1 pu on the active power reference of substation 1 P_{AC1ref} at $t=0.1s$.

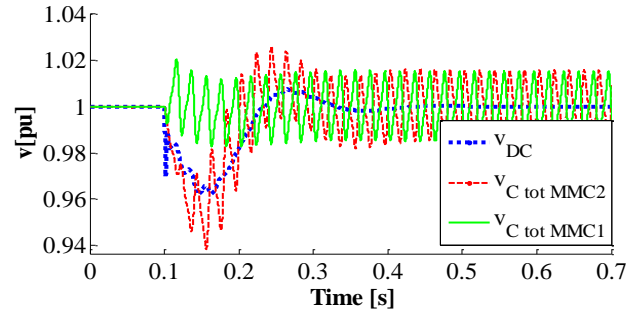


Figure 10: Simulation results for Case A: $S_{K1} = 1$, $S_{K2} = 2$ and $K=1$

Fig. 10 shows that the $v_{CtotMMC1}$ is constant, contrary to $v_{CtotMMC2}$, which depends on v_{DC} variations. These results confirm that in case A the stored energy in MMC1 (W_i^Σ) is constant, contrary to the stored energy in MMC2, which is linked to the DC bus voltage

B. Case B: Two stations with $W_{iref}^\Sigma = W_{DC}(S_{K1} = 2)$

When W_{iref}^Σ is related to W_{DC} for both MMC stations, the SM capacitors of the two MMCs participate in the DC bus control. In this case, application of (16) to MMC1 substation results in:

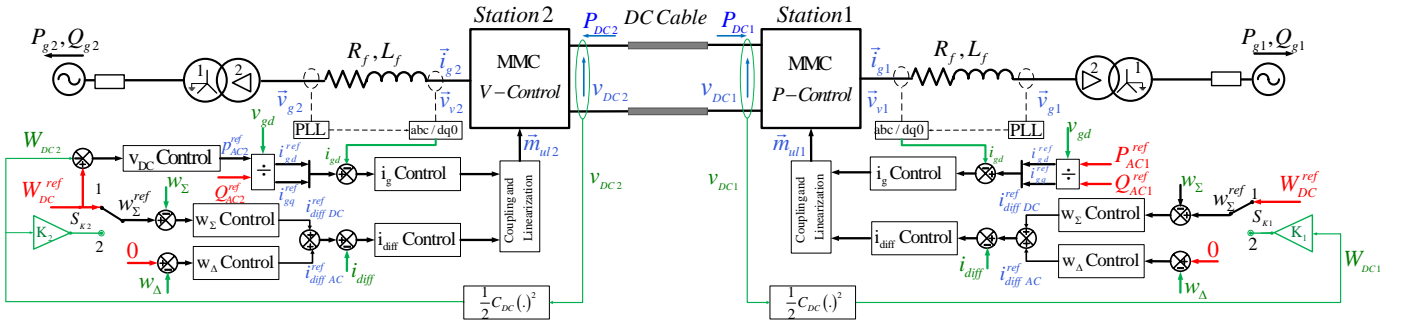


Figure 11: Two terminals HVDC studied case based on MMC substations

$$p_{DC1} = \frac{1}{2} C_{tot} \left(6 \frac{dv_{c tot1 ref}^2}{dt} \right) + P_{AC1 ref} \quad (21)$$

Replacing p_{DC1} in (20) with $W_{i ref 1}^\Sigma = W_{DC}$ leads to:

$$\frac{1}{2} (6C_{tot MMC1} + 6C_{tot MMC2} + C_{DC}) \frac{dv_{DC}^2}{dt} = -p_{AC2 ref} - P_{AC1 ref} \quad (22)$$

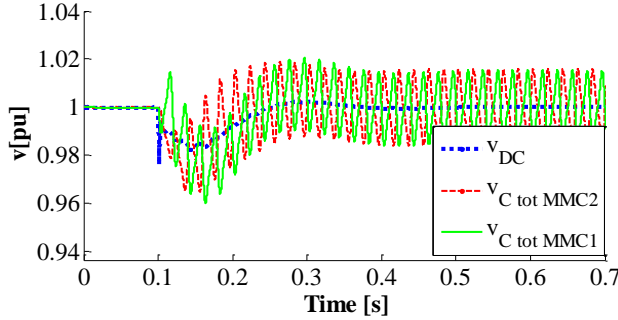
Figure 12: Simulation results for Case B: $S_{K1} = 1$, $S_{K2} = 2$ and $K=1$.

Fig.11 shows that $v_{c tot MMC1}$ and $v_{c tot MMC2}$ depend on v_{DC} variations and the stored energy of both converters participate in DC-bus voltage regulation. It can be observed that the DC-bus voltage drop in this case has been greatly reduced compared with the previous case studied.

C. Case C: Two stations with $W_{i ref}^\Sigma = KW_{DC}$ ($S_{K1} = 2$) and $K=1.21$

The idea of providing an exchange of energy between MMC and DC-bus can be extended by increasing the MMC stored energy using a larger gain K. The value of the gain is limited to avoid an overvoltage on the SMs. For example, if $K=1.21$ the steady state voltage is $v_{c tot} = 1.1 pu$ which may be considered as acceptable. DC bus voltage variation in this case is obtained by considering the gain K in (22) as:

$$\frac{1}{2} (6KC_{tot MMC1} + 6KC_{tot MMC2} + C_{DC}) \frac{dv_{DC}^2}{dt} = -p_{AC2 ref} - P_{AC1 ref} \quad (23)$$

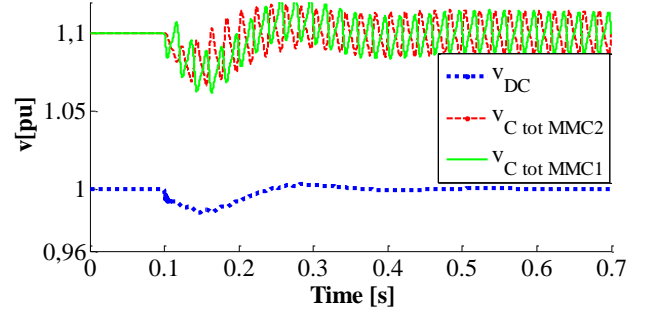
Figure 13: Simulation results for Case C: $S_{K1} = 2$, $S_{K2} = 2$ and $K=1.21$

Fig. 13 shows that there is more stored energy in MMC as $v_{c tot} = 1.1 pu$, in comparison with the two previous cases. Moreover, a slightly reduced voltage drop can be noticed by increasing the participation of the MMC energy to the voltage regulation.

A comparison between the three studied cases is provided in Fig. 14

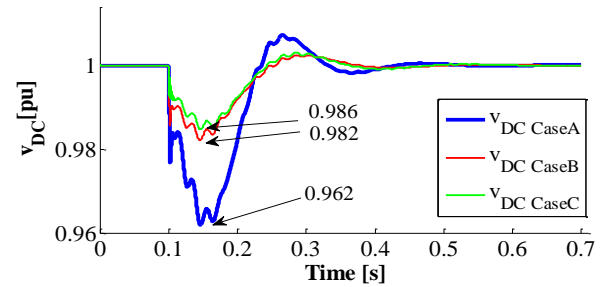


Figure 14: comparison of the Dc-bus voltage in three studied cases

In Fig. 14, it can be seen that the response time is nearly the same since the DC voltage controller has been adjusted as per the DC equivalent capacitor defined in (20), (22) and (23). When comparing Case A and case B, the DC voltage drop decreased significantly in Case B. As depicted in Fig.14, in case B the DC voltage drop is about 1.8% whereas in case A it is about 3.8%.

Moreover, an additional decrease of DC bus voltage drop can be considered, as shown in case C in Fig. 14. In case C, when $K=1.21$ the MMC stored energy increases by 20%, which leads to a DC voltage drop of 1.6%. When comparing Case B and Case C, the DC voltage drop in case C decreases by 10%.

VII. CONCLUSION

The idea proposed in this paper is based on an in-depth analysis of the energy exchanged between the MMC and the DC bus voltage. A degree of freedom has been clearly highlighted in terms of the management of the stored energy since this energy is not directly linked to the DC bus voltage level like in a classical VSC substation.

In case of a non-energy based control, the natural link between the energy and the DC voltage level removes this degree of freedom. In case of an energy-based control, this degree of freedom has not been studied much until now since most of the papers address constant DC bus voltage. As shown in the simulation results, good management of this degree of freedom has an important impact on the dynamic behavior of an HVDC link. Many developments can be proposed from this idea. The very simple relation between the energy and DC bus voltage proposed can be more complex in order to continue improving the dynamic behavior of the HVDC link. These considerations can also be extended to a Multi Terminal DC grid where the stored energy on the DC grid plays a key role on DC bus stability.

REFERENCES

- [1] S. Allebrod, R. Hamerski, and R. Marquardt. "New transformerless, scalable modular multilevel converters for hvdc-transmission". in Proc. IEEE Power Electron. Spec. Conf., pp. 174–179, Jun. 2008.
- [2] A. Lesnicar and R. Marquardt. "An innovative modular multilevel converter topology suitable for a wide power range." Presented at the IEEE Power Tech. Conf., Bologna, Italy, Jun. 2003.
- [3] Q. Tu and Z. Xu. "Impact of sampling frequency on harmonic distortion for modular multilevel converter". IEEE Trans. Power Del., vol. 26, no.1, pp. 298–306, Jan 2011..
- [4] S. Debnath, J. Qin, B. Bahrani, M. Saeedifard, and P. Barbosa. "Operation, control, and applications of the modular multilevel converter: A review". IEEE Trans. Power Tech. vol. 30, no. 1, pp.37–53, 2015.
- [5] Q. Tu, Z. Xu, and L. Xu. "Reduced switching-frequency modulation and circulating current suppression for modular multilevel converters". IEEE Trans. Power Del., vol. 26, no.3, pp. 2009–2017, Jul.2011.
- [6] Y. Zhang, Q. Ge, R. Zhang, and Y. Du. "The control of arm currents and the parameters for modular multilevel converters". In Proc. 15th Int. Electrical Machines and Systems (ICEMS) Conf, pp. 1–6, 2012.
- [7] M. Hagiwara, H. Akagi, "Control and experiment of pulsewidth-modulated modular multilevel converters". IEEE Trans. Power Electron., vol. 24, no.7, pp. 1737–17466, Jul 2009.
- [8] L. Angquist, A. Antonopoulos, D. Siemaszko, K. Ilves, M. Vasiladiotis, and H.-P. Nee. "Open-loop control of modular multilevel converters using estimation of stored energy". IEEE Trans. Ind. Appl., vol. 47, on. 6, pp. 2516–2524, 2011.
- [9] P. Delarue, F. Gruson, and X. Guillaud. "Energetic macroscopic representation and inversion based control of a modular multilevel converter". Presented at the 15th Eur. Conf. power Electron. Appl., pp. 1–10. Lille, France 2013.
- [10] G. Bergna, A. Garces, E. Berne, Ph. Egrot, A. Arzandé, J.-C. Vannier, and M. Molinas. "A generalized power control approach in abc frame for modular multilevel converter hvdc links based on mathematical optimization". IEEE Trans. Power Del., vol. 29, no.1, pp. 386–394, 2014.
- [11] G. Bergna, P. Egrot, E. Berne, P. Lefranc, A. Arzandé, J.-C. Vannier, M. Molinas, "An energy-based controller for HVDC modular multilevel converter in decoupled double synchronous reference frame for voltage oscillations reduction". IEEE Trans. Ind. Electron. vol. 60, no. 6, pp. 2360–2371, Jun., 2012.
- [12] M. Saeedifard and R. Iravani. "Dynamic performance of a modular multilevel back-to-back HVDC system". IEEE Trans. Power Del., vol. 25, no.4, pp. 2903–2912, Oct. 2010.
- [13] F. Xu, Z. Xu, H. Zheng, G. Tang, and Y. Xue. "A tripole hvdc system based on modular multilevel converters". IEEE Trans. Power Del., vol. 29, no.4, pp. 1683–1691, 2014.
- [14] G. Bergna, M. Boyra, and J.-H. Vivas. "Evaluation and proposal of MMC-HVDC control strategies under transient and steady state conditions". Presented at the 14th Eur. Conf. power Electron. Appl., vol. 30, pp. 1–10, 2011.
- [15] S. Denetiere J. Mahseredjian J. Jatskevich J. A. Martinez A. Davoudi M. Saeedifard V. Sood X. Wang J. Cano H. Sassd, J. Peralta and Ali mehrizi Sani. "Dynamic averaged and simplified models for mmc-based HVDC transmission systems". IEEE Trans. Power Del., vol. 28, no.3, pp. 1723–1730, Jul. 2013.
- [16] J. Peralta, H. Saad, S. Denetiere, J. Mahseredjian, and S. Nguefeu. "Detailed and averaged models for a 401-level MMC-HVDC system". IEEE Trans. Power Del., vol. 27, no.3, pp. 1501–1508, 2012.
- [17] A. Antonopoulos, L. Angquist, and H.-P. Nee. On dynamics and voltage control of the modular multilevel converter. Presented at the Eur. Conf., Power Electron. Appl., Barcelona, Spain, 2009.
- [18] S Samimi, P Delarue, F Gruson, and X. Guillaud. "Synthesis of different types of energy based controllers for modular multilevel converter integrated in an hvdc link". In AC and DC Power transmission, 11th IET International Conference IEEE, 2015.
- [19] S Samimi, P Delarue, F Gruson, and X. Guillaud. "Control of dc bus voltage with a modular multilevel converter". In PowerTech., IEEE Eindhoven., 2015.
- [20] M. Hagiwara, H. Akagi, and R. Maeda. "Control and analysis of the modular multilevel cascade converter based on double-star chopper-cells (mmcc-dsc)". IEEE Trans. Power Electron. vol. 26, no. 6, pp. 1649–1658, 2011.
- [21] J. Mahseredjian, S Denetiere, L. Dubé, B. Khodabakhchian, and L. Gérin-Lajoie. "On a new approach for the simulation of transients in power systems". Elect. Power Syst. Res., vol. 77, no. 11, pp. 1514–1520, Sep. 2007.
- [22] L. Harnefors, A. Antonopoulos, S. Norrga, L. Angquist, and H. Nee. "Dynamic analysis of modular multilevel converters". IEEE Trans. Ind. Electron. vol. 60, no. 7, pp. 2526–2537 2012.
- [23] H. Saad, S. Denetiere, J. Mahseredjian, P. Delarue, X. Guillaud, J. Peralta, and S. Nguefeu. "Modular multilevel converter models for electromagnetic transients". IEEE Trans. Power Del., vol. 29, no.3, pp. 1481–1489, 2014.